

## Experimental Investigation of Heat Transfer Enhancement and Flow with Ag, TiO<sub>2</sub> ethylene Glycol distilled Water nanofluid in Horizontal Tube

**Dr. Abdulhassan A. Karamallah**

Machines & Equipments Engineering Department, University of Technology/Bagdad

Email: dr\_ abdulhassank@yahoo.com

**Dr. Khalid F. Sultan**

Electromechanical Engineering Department, University of Technology/Baghdad

### ABSTRACT

The present investigates experimentally the pressure drop and convective heat transfer coefficient of ethylene glycol (EG) and distilled water (DW) based Titanium oxide (TiO<sub>2</sub> (30nm)) and silver (Ag (50nm)) nanofluids in horizontal tube (4mm inner diameter, 6mm outer diameter, and length=2.5m) in the fully developed laminar flow. The concentrations of nanofluid mixture used are ranging from (0.5 – 5% vol). The properties of nanofluids (density, viscosity, thermal conductivity and specific heat) are practically measured. The obtained results show an increase in heat transfer coefficient of 35.4% for TiO<sub>2</sub> + DW, 30.2 % for TiO<sub>2</sub> + (EG + DW), 23.5%, for TiO<sub>2</sub>+ EG and 50.6 % for Ag + DW, 36.2% for Ag + (EG + DW), 25.7 % for Ag + EG. The measured results show that Ag with distilled water nanofluid gives maximum heat transfer enhancement compared with other nanofluid used. As well as the experimental results show that the data for nanofluids friction factor show a good agreement with analytical prediction from the Darcy's equation for single – phase flow. This paper decided that the nanofluid behaviors are close to the typical Newtonian fluids through the relationship between viscosity and shear rate. Moreover to NuR are used to present the corresponding flow and heat transfer inside the tube.

**Keywords:** Nan fluid, Ethylene Glycol, Nur, Enhancement

**التحقيق التجريبي لتحسين انتقال الحرارة والجريان للموائع النانوية باستخدام الفضة وأوكسيد التيتانيوم مع اثيلين كليكول وماء مقطر في أنبوب أفقي**

### الخلاصة

لقد تم قياس معامل انتقال الحرارة و انحدار الضغط لستة أنواع من الموائع الفائقة الدقة وهي TiO<sub>2</sub>+DW, TiO<sub>2</sub>+ (EG+DW), TiO<sub>2</sub>+EG, Ag+ DW, Ag+ (EG +DW), Ag+ EG التشكيل في انبوب افقي القطر الداخلي (4mm) والقطر الخارجي (6mm) وبطول (2.5m). وقد تمت الدراسة لستة أنواع من الموائع الفائقة الدقة مع مدى تراكيز للجزيئات النانوية يتراوح ما بين (0.5 – 5 vol %) كما وتم قياس الخواص الحرارية – الفيزيائية عمليا لهذه الموائع النانوية وهذه الخواص هي اللزوجة والحرارة النوعية, الموصلية الحرارية, الكثافة وأوضح الدراسة أيضا مقدار الزيادة في نسب عدد نسلت لستة أنواع من الموائع الفائقة وهي اوكسيد التيتانيوم مع الماء المقطر, اوكسيد التيتانيوم مع الماء المقطر واثيلين كليكول , اوكسيد

التيتانيوم مع اثيلين كلايكول, الفضة مع الماء المقطر, الفضة مع الماء المقطر واثيلين كلايكول, الفضة مع اثيلين كلايكول, وهذه النسب كانت بالتتابع (35.4%, 30.2%, 23.5%, 50.6%, 36.2%, 25.7%). وبينت النتائج العملية ان الفضة يعطي اكثر تحسین في انتقال الحرارة من باقي الموائع النانوية المستخدمة. وبينت الدراسة العملية أن قيم معامل الاحتكاك تتوافق جيدا مع القيم المستخرجة من معادلة دارسي لجريان أحاديالطور. أن الموائع الفائقة الدقة هي موائع نيوتينية من خلال العلاقة الخطية بين اللزوجة ومعدل القص. بالإضافة إلى العامل NuR استخدم لإظهار مجال الجريان وانتقال الحرارة داخل الأنابيب.

## INTRODUCTION

Nano fluids, which contain nanoparticles dispersed in base fluids, have been proposed as a new kind of heat transfer media because they can improve the heat transport and energy efficiency and may have potential applications in the field of heat transfer enhancement. The thermal conductivity of the Nanofluids can be enhanced obviously when Nanoparticles, such as CNTs [1], Fe [2], Cu [3], and Al<sub>2</sub>O<sub>3</sub> [4], are dispersed into the base fluids. Viscosity of the fluids also increases with the augment of the Nanoparticles concentrations [5, 6] when nanoparticles are dispersed into the base fluids as well. At the same time, temperature and nanoparticles size [6] may have effects on the viscosity of the nanofluids. According to the previous studies [7–9], nanofluids can improve the convective heat transfer coefficient considerably comparing to the conventional heat transfer fluids and can be used in thermal devices or systems such as heat exchangers or cooling system to enhance heat transfer. Magnetic fluids, suspension containing magnetic nanoparticles, show both magnetic and fluid properties and have important applications in industrial [10, 11] and biomaterial fields [12–14]. However, seldom experiments and applications on the heat transfer of magnetic fluids have been reported. The conductivity of magnetic Nanofluids could be improved through controlling the alignment of nanoparticles by the external magnetic field [15]. What's more, with the development of the industry and the technology, the performance elevation of the traditional heat transfer medium using mixture of water and ethylene glycol (EG) is necessary. Kulkarni et al. [16] investigated the thermal properties of aluminum oxide nanofluids based on the mixture of EG and water. And they found that the heat transfer was enhanced efficiently. Eastman [17] reported that theca / ethylene glycolnanofluid with 0.3% volume of Cunanoparticles can enhance thermalconductivity up to 40%. There are only fewprevious studies involve in describing fluid flow andconvective heat transfer performance of thenanofluids [18 – 21]. In their study,  $\gamma$ -Al<sub>2</sub>O<sub>3</sub> with mean diameter of 13nm and TiO<sub>2</sub> with mean diameter of 27 nm were dispersed in water, and the experimental results showed that the suspended nanoparticles increased convective heat transfer coefficient of the fluid. Therefore, the convective heat transfer coefficient of the nanofluids is a function of properties, dimension and volume fraction of suspended nanoparticles, and the flow velocity.

The object of this study is to investigate laminar flow convective heat transfer and rheological Properties of Ag and TiO<sub>2</sub> nanoparticles in EG, DW and EG + DW mixture under constant heat flux boundary condition and different concentration of nanoparticles.

### NANOFLUID PREPARATION

The studied nanofluid is formed by silver (Ag (50nm)) and Titanium oxide (TiO<sub>2</sub> (30nm)) nanoparticles and the two – step method was used to prepare nanofluids. Nanofluid samples were prepared by dispersing pre – weighed quantities of dry Particles in three types of the base fluid and these distilled water, ethylene glycol and the mixture of ethylene glycol and distilled water with volumeratio of 60:40. In a typical procedure, the pH of each nanofluid amixture was measured .The mixtures were then subjected to ultrasonic mixing [60 kHz, 150w at 25 – 30C<sup>0</sup>, Toshiba, England] for several minutesto breaks up any nanoparticle aggregates. The acidic pH is much less than the isoelectric point [iep] of these particles, thus ensuring positive surface charges on the particles. The surface enhanced repulsion between the particles, which resulted in uniform dispersions for the duration of the experiments. An imagenanofluids containing Ag (30nm) and Titanium oxide (30nm)is display in Figure (1) Nanofluids with different volume fractions ( $\Phi=0.5, 1, 2, 3$  and 5vol %)



Figure (1) Shows nanofluids for Ag+ EG, TiO<sub>2</sub> + EG and EG.

### EXPERIMENTAL SETUP

The experimental loop was designed for convective heat transfer in laminar flow domain. The horizontal test section was Pyrex tube with an inner diameter (ID) of 4mm and length of 2.5m. The tube surface is electrically heated by coil made from tungsten matter connecting to an AC power supply to generate heat flux. To measure the wall temperature of the Pyrex tube and the bulk mean temperature of the fluids at the inlet and out let of the tube ten thermocouples (T – types) are soldered at place along the test section and two thermocouple (T – types) are inserted at the inlet and out let of the test section. The pressure drop is measured by two gauge pressure. The range pressure operates over range of [0 – 400 mbar] at beginning of the test section and other end the range pressure operates over range [0 – 150 mbar]. To preserve a constant temperature at the inlet of the test section the heated fluid returns to reservoir tank passing spiral Pyrex heat exchanger to a cooler fluid. The flow meter was positioned just after the pump discharge. A schematic diagram and a photograph of

the experimental rig are shown Figures (2, 3) for convective heat transfer and flow characteristics of the nanofluid.



Figure (2) The experimental system of the convective heat transfer and flow characteristics for nanofluid, [33].

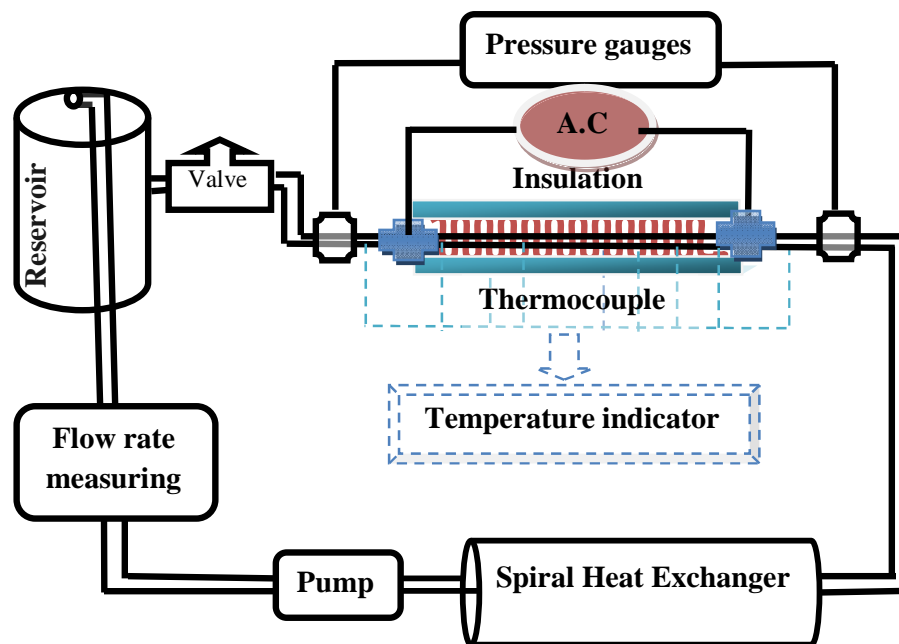


Figure (3) A schematic diagram of the experimental set – up for the convective heat transfer and flow characteristics for nanofluid.

**MEASUREMENT OF THERMAL PROPERTIES NANOFUID**

All physical properties of the ethylene glycol, distilled water, ethylene glycol and distilled water based Ag and TiO<sub>2</sub> nanofluids needed to calculate the pressure drop and the convective heat transfer are measured. The dynamic viscosity ( $\mu$ ) is measured using brook field digital viscometer model DV-E. Figures (4&5). give the comparison between the practical measurement of dynamic viscosity with the empirical relation of Einstein model [22], Brinkman model [23], Wang et model [24] and Batchel model [25]. The thermal conductivity, specific heat and density are measured by Hot Disk Thermal Constants Analyzer (6.1), Brook field digital viscometer model DV-E, specific heat apparatus (ESD – 201) as well as the measurement of density was carried out by weighing a sample and volume. In addition, a measured value of the density agrees well with the values calculated from mixing theory [26] as shown in Figures (7 and 8). The experimental result for thermal conductivity indicated at comparison with the models of thermal conductivity developed by researchers such as Wasp model [27], Hamilton and Crosser model [28], Maxwell model [29] and TimoFeera et al model [30]. The Wasp model is the closest to practical with difference does not exceed 2.15 %. Figures (10, 11) shows the thermal conductivity ratio for EG + DW based TiO<sub>2</sub> and Ag nanofluids. The experimental result for specific heat was compared with two models of specific heat used in all research in this field. The second model is the closest to a practical with a difference of 1.19 % and Figures (13&14) shows comparison with two models [31, 32]. Figures (6, 9, 12 and 15) represent viscosity, density, thermal conductivity and specific heat ratio for the one type of nanoparticles Ag with three types of the base fluids EG, DW, EG + DW. ( $\mu$ ,  $\rho$ ,  $K$  and  $C_p$ ) are increase of about 8.21%, 4.30%, 11.6 % and 1.65% respectively for the first type of nanoparticle while increased about 12.45%, 4.52%, 17.4 % and 6.28% for the second type of nanoparticle at 5vol% and 25 C<sup>0</sup> compared with that of distilled water.

**DATA ANALYSIS AND VALIDATION**

It is necessary to know the heat transfer coefficient used in this study clearly before making any calculations. The local heat transfer coefficient of the equation as follows.

$$h_z = \frac{q}{(\Delta T)_z} \quad \dots (1)$$

Where:  $(\Delta T)_z$  have been taken as the difference between the temperature of the surface localized  $(T_s)_z$  and the temperature of the fluid  $(T_b)_z$  at length Z from the entrance of the tube. Also, with the energy balance in a tube the mean temperature of fluid can be given by

$$(T_b)_z = T_i + \frac{qp}{mCp} Z \quad \dots (2)$$

Where:  $T_i$ ,  $p$ ,  $m$  and  $Cp$  are the fluid temperature at the inlet of test section, the surface perimeter, the mass flow rate and the heat capacity, respectively. Thus the local heat transfer coefficient becomes

$$h_z = \frac{q}{(T_s)_z - (T_b)_z} \quad \dots(3)$$

Therefore, the local heat transfer coefficient can be obtained with Equations (3) and (2). In order to verify the accuracy and the reliability of this experimental system, the pressure drop and the local heat transfer coefficient are experimentally measured using water before obtaining those of EG, DW, EG + DW based silver (Ag (30nm)) and Titanium oxide (TiO<sub>2</sub> (30nm)) nanofluids. The experiments on the pressure drop are conducted within the Reynolds number of 800, and entry length is within 2% of total tube length. Therefore, we can assume the fully developed laminar flow regime. Figure (20). Shows that pressure drop data for water and analytical predictions using Equation (4) have a good agreement with less than 1.5% error.

$$\Delta p = 32 \frac{\mu_m \mu L}{d_{tube}^2} \quad \dots (4)$$

The heat transfer coefficients calculated by Equations (3 and 2) are compared with the following Shah equation [34] of the local Nusselt number in circular tube for a constant heat flux condition according to the Reynolds number in Figure (21).

$$Nu_z = \begin{cases} 1.302 Z^{*\frac{1}{3}} - 1.328 Z^{*\frac{1}{4}} & Z^* \leq 0.00005 \\ 1.302 Z^{*\frac{1}{3}} - 0.5 Z^{*\frac{1}{4}} & 0.00005 \leq Z^* \leq 0.0015 \\ 4.364 + 8.68 (10^3 Z^*)^{-0.506} \exp(-41 Z^*) & Z^* \leq 0.001 \end{cases} \quad \dots (5)$$

Where:  $Nu = \frac{h_z d}{k}$  ,  $Z^* = \frac{2(Z/d)}{Re Pr}$ . For fully developed laminar flow regime,

the experimental data compared with Shah Equation [34] have good agreement within 2% error and are constant. To show the effect of the nanofluids on heat transfer rate, introducing a variable called Nusselt number ratio (NuR) with its definition given as:

$$NuR = \frac{Nu_{ave} | \text{with nanofluid}}{Nu_{ave} | \text{with pure fluid}} \quad \dots (6)$$

If the value of NuR greater than 1 indicated that the heat transfer rate is enhanced on that fluid, whereas reduction of heat transfer is indicated when NuR is less than 1. The Nusselt number is used as an indicator of heat transfer enhancement where an increase in Nusselt number corresponds to enhancement in heat transfer.

## RESULTS AND DISCUSSION

The pressure drop of EG, DW, EG+DW – based TiO<sub>2</sub> and Ag nanofluids flowing through a circular tube is experimentally measured to investigate flow characteristics of the nanofluids. Based on the pressure drop of EG, W, EG+DW – based TiO<sub>2</sub> and Ag nanofluids, we can express the Darcy friction factor, which is dimensionless parameter defined as.

$$f = \frac{\Delta p}{\rho U_m^2 / 2} \quad \dots (7)$$

For fully developed laminar flow, it follows that

$$f = \frac{64}{\text{Re}_{\text{D tube}}} \quad \dots (8)$$

Substituting the pressure drop into Equation (7), the Darcy friction factor can be calculated. Figures (18 – 23). Shows that the Darcy friction factor of TiO<sub>2</sub>, Ag and EG, DW, (EG+DW) base nanofluids in fully developed laminar flow regime has a good agreement with results of Equation (8) with less than 2% error. This implies that the friction factor correlation for single – phase flow can be extended to EG, DW and (EG+DW) based TiO<sub>2</sub> and Ag nanofluid. The wall temperature and nanofluid temperature to TiO<sub>2</sub>, Ag and EG, DW, (EG+DW) base nanofluids flowing through a circular tube for a constant heat flux is experimentally measured to understand convective heat transfer characteristics of TiO<sub>2</sub>, Ag and EG, DW, (EG+DW) base nanofluids. Figures ( 24, 26, 28 ) DW, EG, (EG+DW) – based TiO<sub>2</sub> and Figs.(25, 27, 29) DW, EG and EG +DW based Ag shows the Nusselt number for six types of nanofluids as function of non – dimensional axial distance at different Rayleigh number for volume fraction 5 vol%. The experimental results clearly show that nanoparticles suspended in DW, EG, EG+DW enhance the heat transfer and the local Nusselt number of nanofluids increases with volume fraction of TiO<sub>2</sub> and Ag nanoparticles as shown in Figures.( 24, 26, 28 ) and Figures (25, 27, 29).

The study also demonstrated that the increase in Nusselt number for the six types of nanofluid are respectively (35.4%, 30.2 %, 23.5%, 50.6 %, 36.2%, 25.7 %) compared with that distilled water. It should be noted that the enhancement of heat transfer greatly depend on particle type, particles size, base fluid and flow regime. Nanofluids that contain metal nanoparticles Ag (50nm) + EG, Ag (50nm) +DW, Ag (50nm) + (EG+DW) show more enhancement compared with oxide nanofluids TiO<sub>2</sub> (30nm) + EG, TiO<sub>2</sub> (30nm) + DW, TiO<sub>2</sub> (30nm) + (EG+DW). The oxide of nanofluids present fewer enhancements in local Nusselt number at same nanoparticle concentration. It is related to large particle size, high viscosity and high thermal conductivity of Ag (50nm) + EG, Ag (50nm) +DW, Ag (50nm) + (EG+DW). NuR is used to present the corresponding flow and heat transfer inside the tube.

Figures (30 – 35) represent viscosity versus shear rate for six types of nanofluid in various concentrations. It can be found that there is almost linear relation between viscosity and shear rate for all concentrations of nanofluids which confirm a Newtonian behavior for TiO<sub>2</sub> and Ag in volume fraction 0.5 – 5 vol %. Some theoretical predictions of viscosity, Einstein model, Brinkman model, Wang et model and Batchel model, about the fluid were employed to compare with experiments of

the nanofluids in Figures (4&5). It is found that the experimental data of the nanofluids is much larger than the theoretical predictions values. The result may ascribe to the specific surface areas of the nanoparticles. The enhancement of viscosity may due to the very large surface area of the nanoparticles in the nanofluids. Furthermore, the reason of the discrepancy may due to the nanoparticles size, which has an important effect on viscosity of nanofluids. When the diameter of the nanoparticles is less than 20 nm, the viscosity of nanofluids will increase rapidly as the diameters decrease. Figure (6) depicts the rheological behaviors of the nanofluids with different particle loadings. The behaviors of the nanofluids from this Figs are close to the typical Newtonian fluids. Yu et al. measured the viscosity of ZnO/EG nanofluids against shear rate. The results also showed that the viscosity of nanofluids increased with the increasing of nanoparticle concentrations. Figure (36) indicated enhancement ratio of heat transfer for six types of the nanofluids.

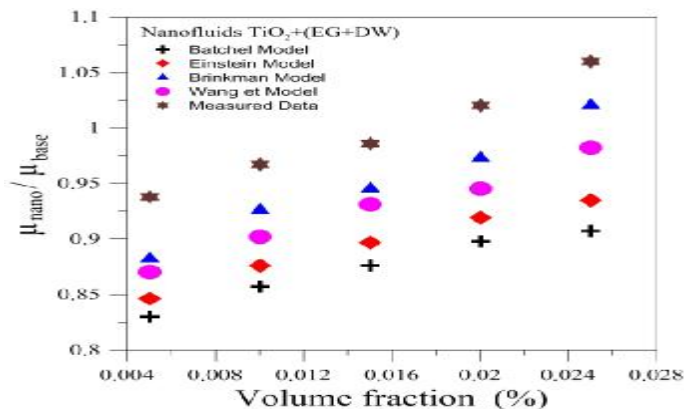


Figure (4) Viscosity ratio for TiO<sub>2</sub>+ (EG+DW).

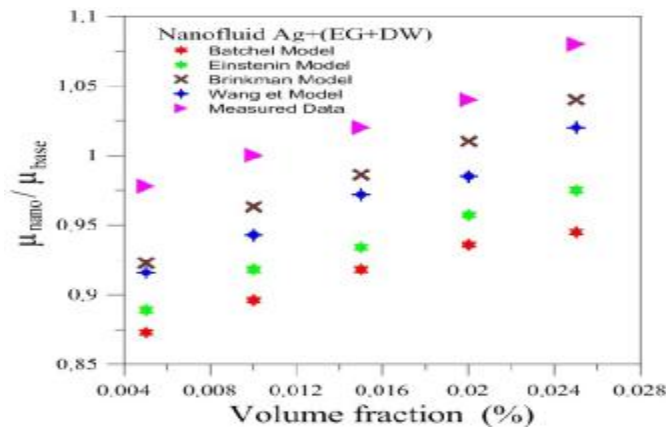


Figure (5) Viscosity ratio for Ag+ (EG+DW).

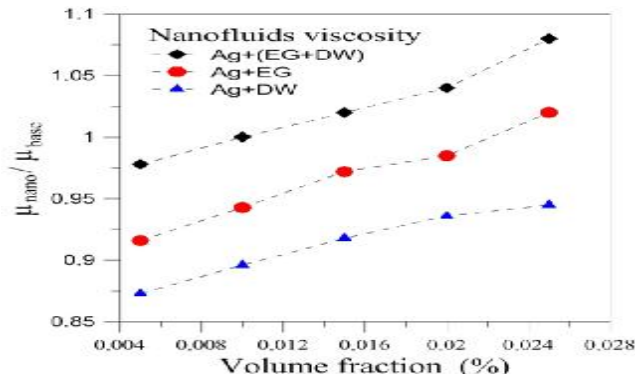


Figure (6) Three types of viscosity ratio for Ag.

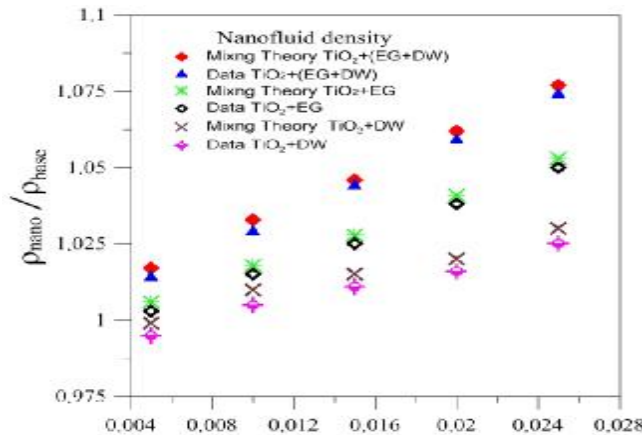


Figure (7) Comparison density ratio with Mixing theory for TiO<sub>2</sub>.

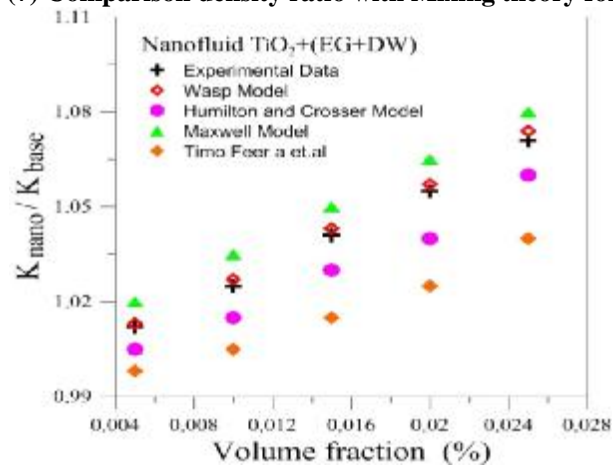


Figure (8) Comparison density ratio with mixing.

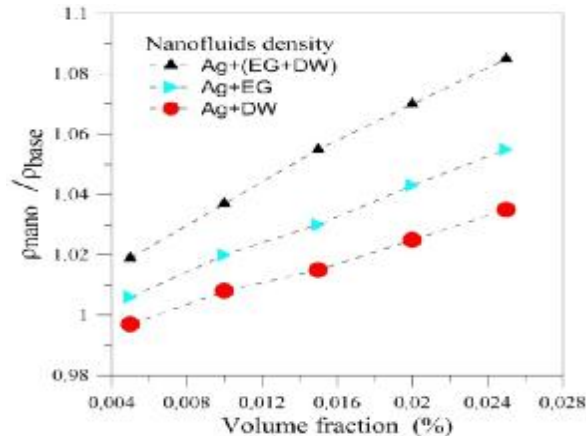


Figure (9) Three types of density ratio for Ag.

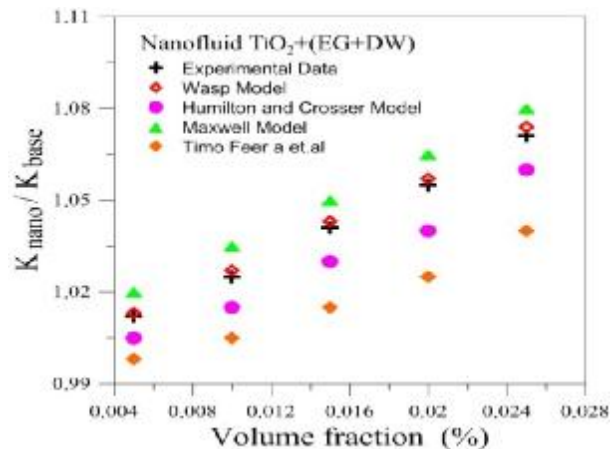


Figure (10) Thermal conductivity ratio for TiO<sub>2</sub> + (EG+DW).

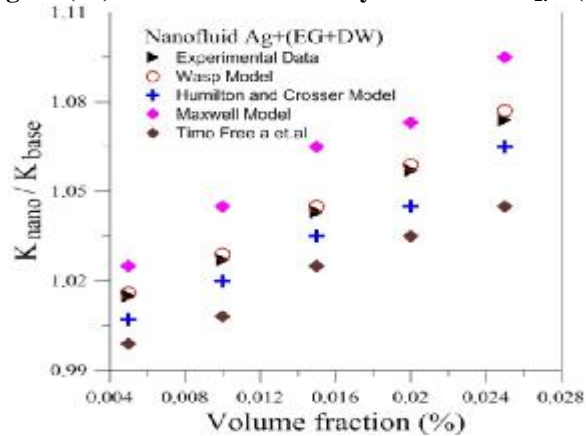


Figure (11) Thermal conductivity ratio for Ag+ (EG+DW).

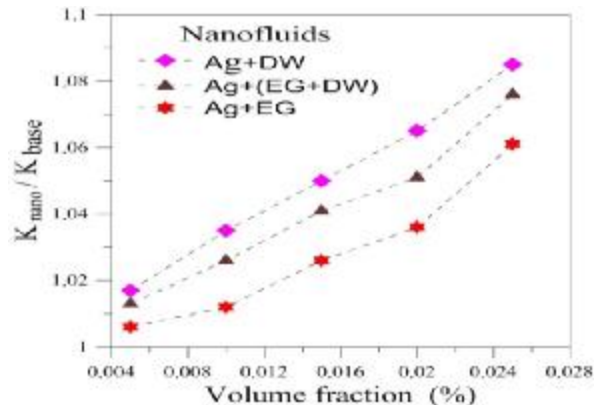


Figure (12) Three types of thermal conductivity Ratio for Ag.

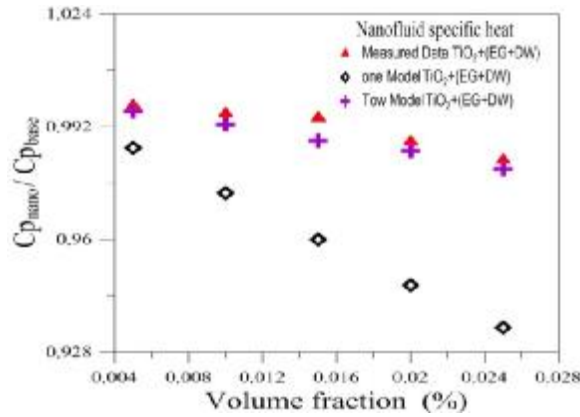


Figure (13) Specific heat ratio for  $TiO_2 + (EG+DW)$ .

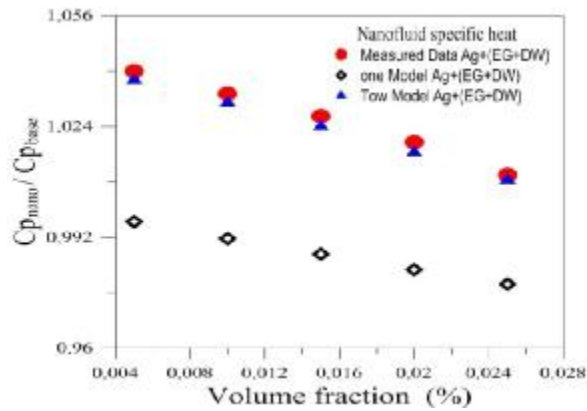


Figure (14) Specific heat ratio for Ag+ (EG+DW).

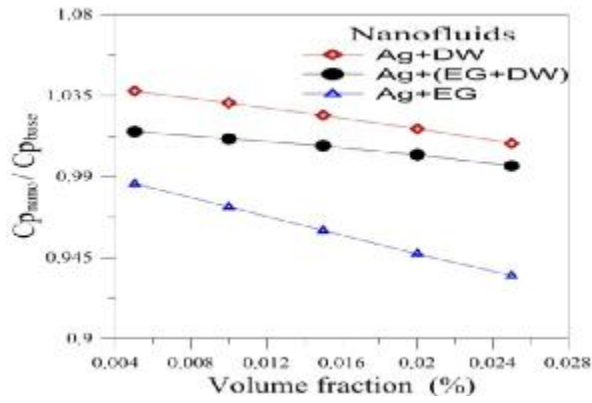


Figure (15) three types of specific heat ratio for Ag.

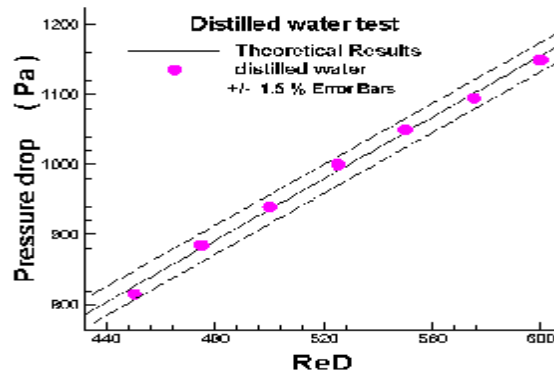


Figure (16) Comparison between theoretical and Experimental pressure drops of water.

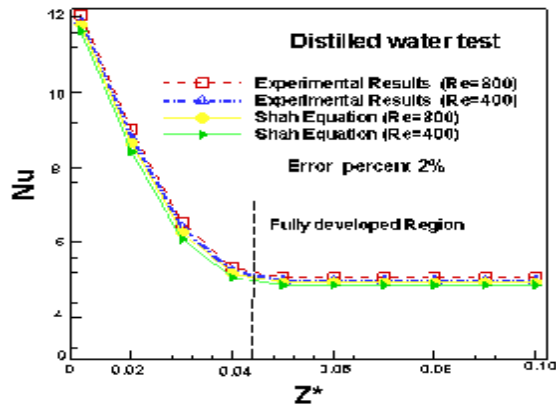


Figure (17) Comparison between Shah Equation and Experimental data for convective heat transfer.

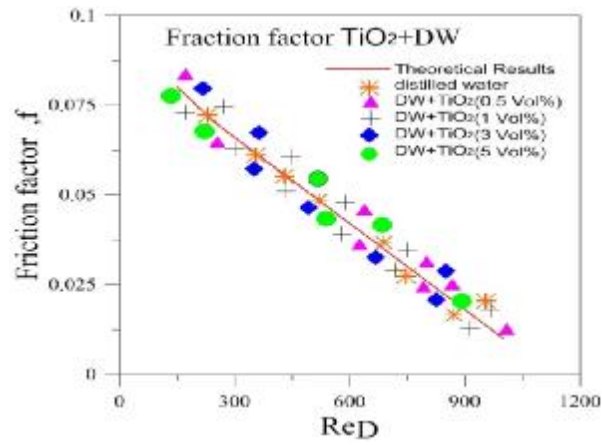


Figure (18) The friction factor of TiO<sub>2</sub>+DW nanofluid in fully developed laminar flow.

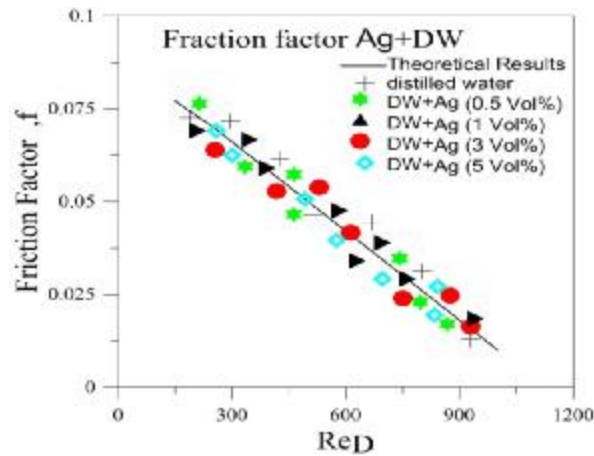


Figure (19) The friction factor of Ag +DW nanofluid in fully developed laminar flow.

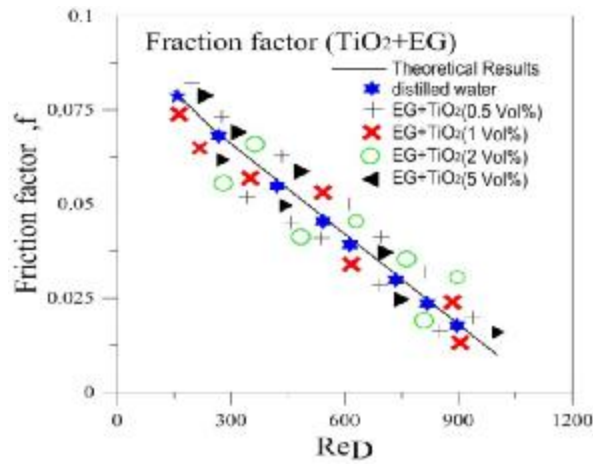


Figure (20) The friction factor of TiO<sub>2</sub> + EG nanofluid in fully developed laminar flow.

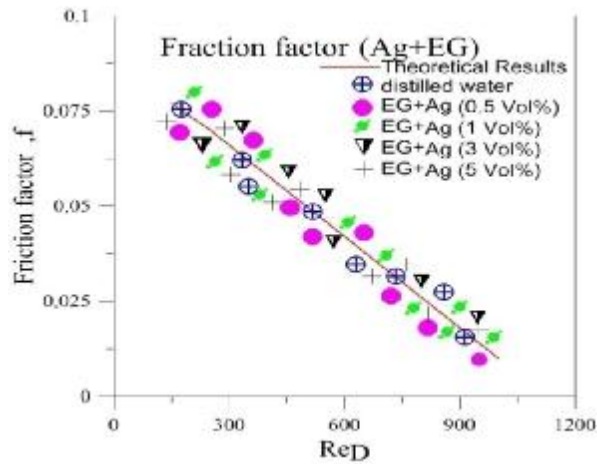


Figure (21) The friction factor of Ag + EG Nanofluid in fully developed laminar flow.

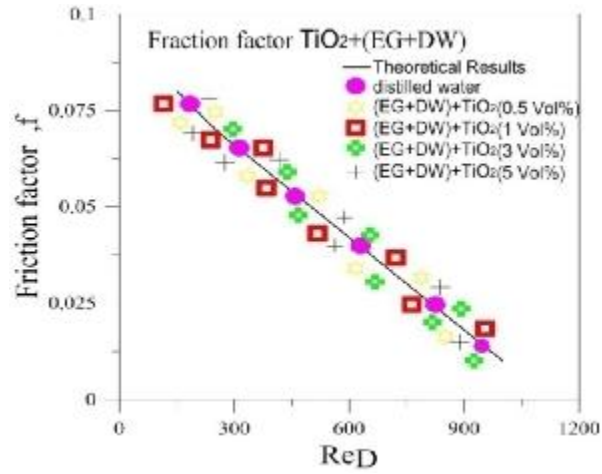


Figure (22) The friction factor of  $TiO_2$  + (EG +DW) Nanofluid in fully developed laminar flow.

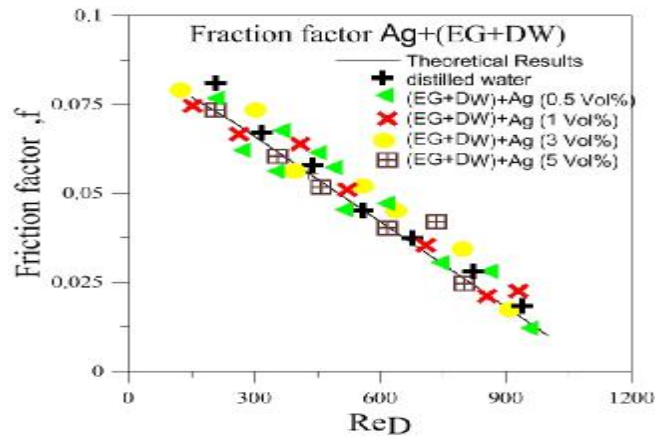


Figure (23) The friction factor of Ag + (EG+ DW) Nanofluid in fully developed laminar flow.

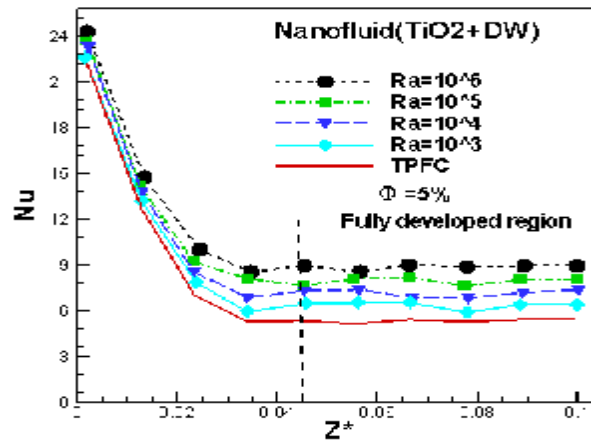


Figure (24) The Local Nusselt number of TiO<sub>2</sub>+DW Nanofluid at Φ = 5 vol % and different Ra.

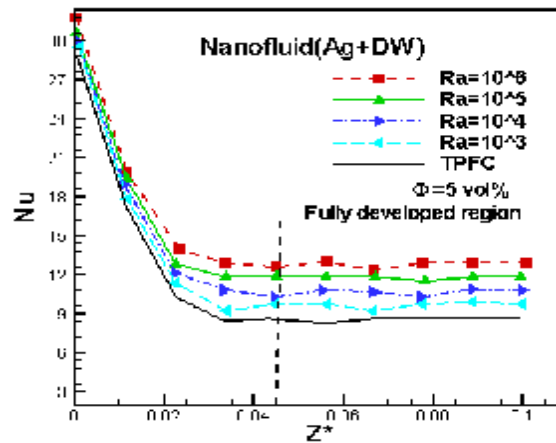


Figure (25) The local Nusselt number of Ag+ DW nanofluid at Φ = 5 vol % and different Ra.

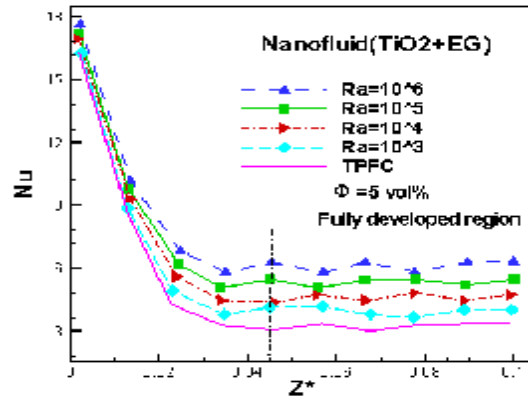


Figure (26) The local Nusselt number of TiO<sub>2</sub>+ EG Nanofluid at  $\Phi = 5$  vol % and different Ra.

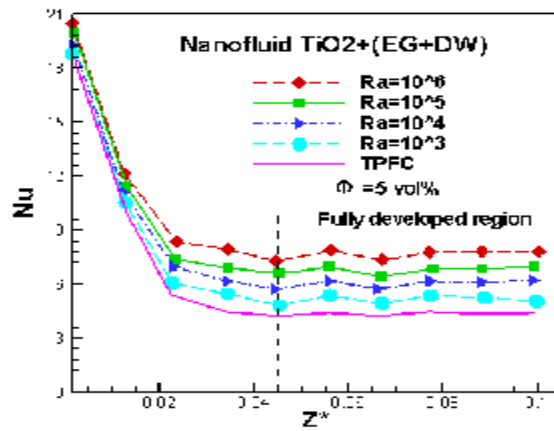


Figure (27) The local Nusselt number of Ag+ EG nanofluid at  $\Phi = 5$  vol % and different Ra.

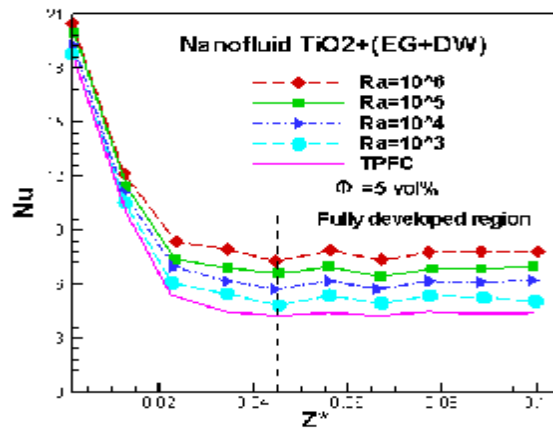


Figure (28) The local Nusselt number of  $TiO_2+(EG+DW)$ .

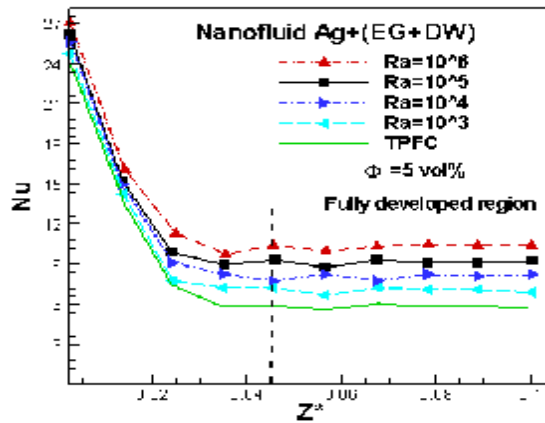


Figure (29) The local Nusselt number of Ag+(EG+DW) nanofluid at  $\Phi = 5 \text{ vol } \%$  and different Ra.

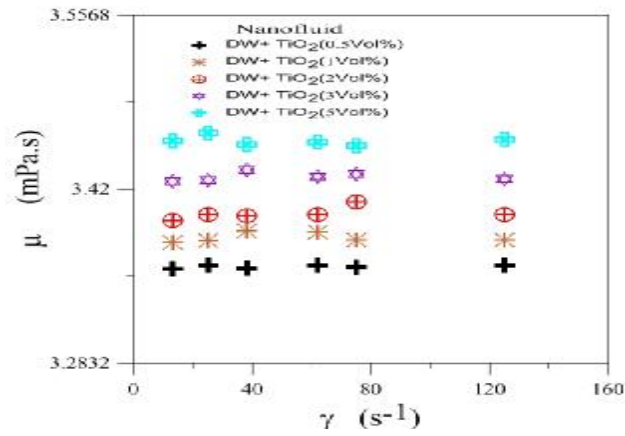


Figure (30) Viscosity as a function of shear rate for TiO<sub>2</sub>+ DW Nanofluid Ag+ DW nanofluid.

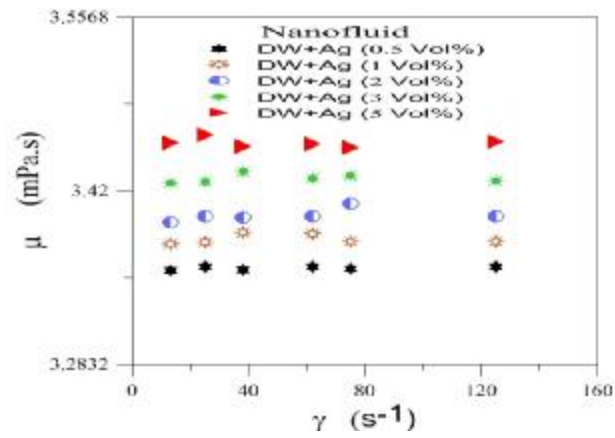


Figure (31) Viscosity as a function of shear rate for nanofluid at  $\Phi = 5$  vol % and different Ra.

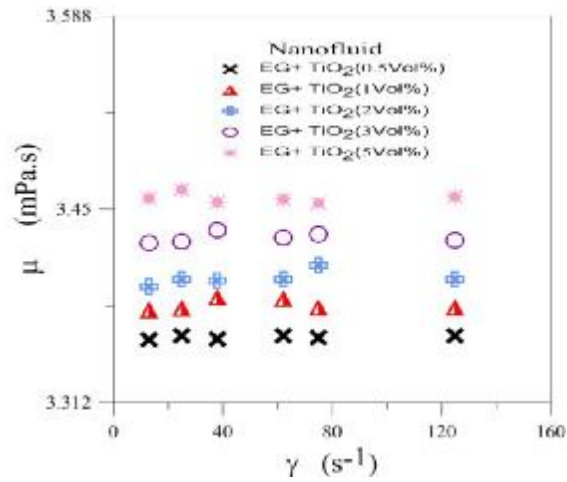


Figure (32) Viscosity as a function of shear rate For TiO<sub>2</sub>+EG nanofluid.

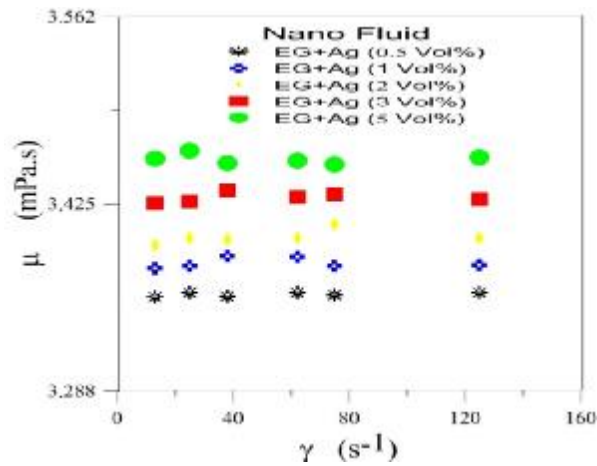


Figure (33) Viscosity as a function of shear rate for Ag+ EG nanofluid.

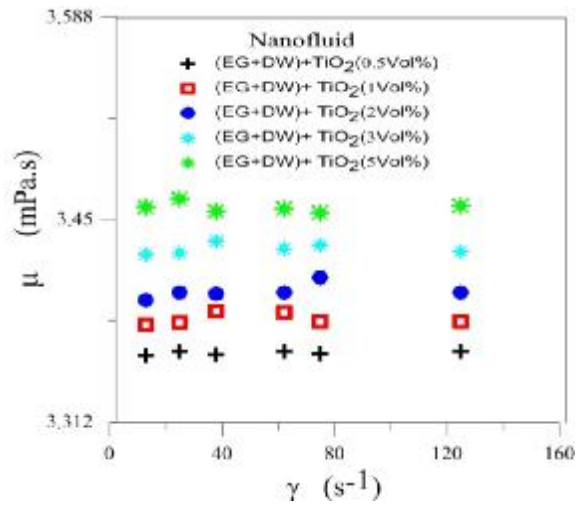


Figure (34) Viscosity as a function of shear rate for TiO<sub>2</sub>+ (EG+DW) nanofluid.

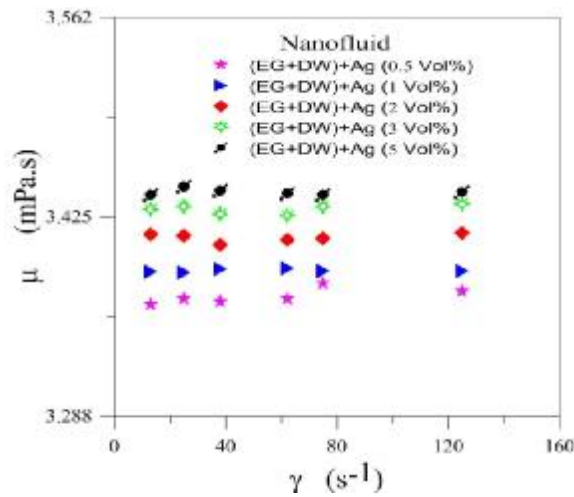


Figure (35) Viscosity as a function of shear rate for Ag+ (EG+DW) nanofluid.

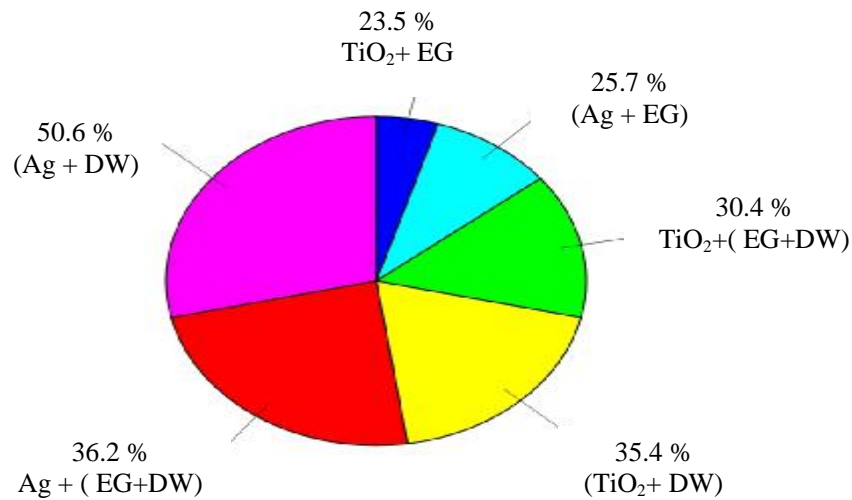


Figure (36) Enhancement ratio of heat transfer for six types of the nanofluids.

### CONCLUSIONS

The conclusions can be drawn from the results of experimental study were as follows:

1. The nanofluid has larger heat transfer (Nusselt number) than distilled water and ethylene glycol under the same Reynolds number.
2. The type and base fluid to nanofluid is a key factor for heat transfer enhancement. The high values are obtained when using Ag and TiO<sub>2</sub> nanoparticles respectively.
3. NuR increase generally with Ra at constant  $\Phi$  and increases with  $\Phi$  at constant Ra.
4. Heat transfer enhances with increasing nanoparticles concentration.
5. Nanofluids that contain metal nanoparticles (Ag) show more enhancements compared to oxide nanofluids TiO<sub>2</sub>+ EG, TiO<sub>2</sub>+DW and TiO<sub>2</sub>+ (EG+DW).
6. There is an optimum concentration for each nanofluid in which more enhancement are available. It is related to viscosity increasing by particle concentration.
7. It is found that the nanofluids Nusselt number enhancement is not only due to the increase of thermal conductivity but also due to other factors such as nanofluid viscosity, base fluid.
8. The nanofluid will not cause a penalty in pressure drop and there is no need for pump power. This may be because the small additional nanoparticles in the base liquid do not cause the change in the flow behavior of the fluid. The pressure drop to base fluid of ethylene glycol smaller than the base fluid of distilled water.

**REFERENCES**

- [1]. Chen, L.F. H.Q. Xie, Y. Li, W. Yu, *Thermochim. Acta* (2008) , 477, 21.
- [2]. Hong, T.K. H.S. Yang, C.J. Choi, *J. Appl. Phys.* 97, , (2005) ,064311.
- [3]. Garg, J. B. Poudel, M. Chiesa, J.B. Gordon, J.J. Ma, J.B. Wang, Z.F. Ren, Y.T. Kang, H. Ohtani, J. Nanda, G.H. McKinley, G. Chen, *J. Appl. Phys.* ,(2008)103, 074301.
- [4]. Xie, H.Q. J.C. Wang, T.G. Xi, Y. Liu, F. Ai, Q.R. Wu, *J. Appl. Phys.*,(2002),91(7), 4568 .
- [5]. Namburu, P.K. D.P. Kulkarni, D. Misra, D.K. Das, *Exp. Therm.Fluid Sci.* ,(2007), 32, 397.
- [6]. Nguyen, C.T. F. Desgranges, N. Galanis, G. Roy, T. Mare´d,S. Boucher, H.A. Mintsas, *Int. J. Therm. Sci.* (2008),47, 103,
- [7]. Maiga, S.E.B. C.T. Nguyen, N. Galanis, G. Roy, *Superlattices Microstruct.* ,(2004),35, 543 .
- [8]. Heris, S.Z. S.G. Etemad, M.N. Esfahany, *Int. J. Heat Mass Transf.* , (2006),33, 529.
- [9]. Wen, D.S. Y.L. Ding, *Int. J. Heat Mass Transf.* (2004), 47, 5181.
- [10]. Bhimani, Z. B. Wilson, *Ind. Lubr. Tribol.* ,(1997) ,49, 288.
- [11]. Hatch, A. A.E. Kamholz, G. Holman, P. Yager, K.F. Bo¨hringer, *J. Microelectromech. Syst.* (2001), 10(2), 215.
- [12]. Jiang, J.S. Z.F. Gan, Y. Yang, B. Du, M. Qian, P. Zhang, *J. Nanopart. Res.* (2009), 11, 1321.
- [13]. Gan, Z.F. J.S. Jiang, Y. Yang, B. Du, M. Qian, P. Zhang, *J. Biomed. Mater. Res.* (2008), 84A, 10.
- [14]. Yang, Y. J.S. Jiang, B. Du, Z.F. Gan, M. Qian, P. Zhang, *J. Mater. Sci. Mater. Med.* (2009),20(1), 301.
- [15]. Philip, J. P.D. Shima, B. Raj, *App. Phys. Lett.* (2008) ,92, 043108.
- [16]. Kulkarni, D.P. R.S. Vajjha, D.K. Das, D. Oliva, *Appl. Therm.Eng.* (2008),28, 1774.
- [17]. Eastman, J.A., Choi S.U.S., Li S., Yu W.,Thompson L.J., Anomalous increase in effective thermal conductivities of ethylene glycol – based nanofluids containing copper nanoparticles, *Applied Physics letters* ,(2001),78 (6), 718 – 720.
- [18]. Xuan, Y. W. Roetzel, Conception for heat transfer correlation of Nano fluid, *Int. J. Heat Mass Transfer* (2000), 43 (19) ,3701 – 3707.
- [19]. Xuan, Y. Q. Li, Investigation on convective heat transfer and flow features of nanofluids, *J. Heat Transfer* (2003),125 ,151 – 155.
- [20]. Wen, D. Y. Ding, Experimental investigation into convective heat transfer of nano fluid at the entrance rejoin under laminar flow conditions, *Int. J. Heat Mass Transfer* (2004), 47 (24) ,5181 – 5188.
- [21]. Yang, Y. Z.G. Zhang, E.A. Grulke, W.B. Andersen, G. Wu, Heat transfer properties of nanoparticle in fluid dispersions (nanofluids)in laminar flow, *Int. J. Heat Mass Transfer*, (2005), 48(6) 1107 – 1116.
- [22]. Einstein, A. Investigation on the theory of Brownian motion, Dover, New York, (1956),pp.1 – 18.
- [23]. Binkman, H.C. The viscosity of concentrated suspensions and solution. *Chem. Phys* (1952), 20,571.

- [24]. Wang, X. X.Xu, S.U.S.Choi, Thermal conductivity of nanoparticle –fluid mixture. *Thermo phys. Heat transfer*, (1999), 13, 474 – 480.
- [25]. Batchelor, G.K. The effect of Brownian motion on the bulk stress in a suspension of spherical particles. *J.Fluid mech.*, (1977), 83 (1), 97.
- [26].Smith,J.M. H.C. Van Ness, *Introduction to Chemical Engineering Thermodynamic*, McGraw-Hill, New York, (1987).
- [27]. Wasp, E.J. J.P. Kenny, R.L. Gandhi, *Solid–liquid Slurry Pipeline Transportation, Bulk Materials Handling*, Trans Tech Publications, Germany,(1999).
- [28]. Hamilton, R.L. and O.K. Crosser, Thermal Conductivity of Heterogeneous 2-Component Systems.*Industrial & Engineering Chemistry Fundamentals*, 1(3): p.(1962), 187.124.
- [29]. Maxwell, J.C. *A Treatise on Electricity and Magnetism*, second ed., Clarendon Press, Oxford, UK, (1881).
- [30]. Timofeeva, E.V., A.N. Gavrilov, J.M. McCloskey, Y.V. Tolmachev, S. Sprunt,L.M. Lopatina, and J.V. Selinger, Thermal conductivity and particle agglomeration in alumina nanofluids: Experiment and theory. *Physical Review E*, 76(6): p. 16, (2007).
- [31]. Xuan, Y. W. Roetzel, Conceptions for heat transfer correlation of nano fluids, *Int. J. Heat Mass Transfer* (2000), 43 3701–3707.
- [32]. Pak, B.C. Y.I Cho, Hydrodynamic and heat transfer study of dispersed fluids with sub micro metallic oxide particles, *Exp. Heat transfer* ,(1998),11,151.
- [33]. Abdulhassan, Abd. K, Sattar Al – Jabair , Khalid Sultan Experimental investigation of heat transfer, and Flow of nanofluids in horizontal circular tube, *International Journal of Mechanical and Aerospace Engineering* 6,( 2012).
- [34]. Shah, R.K. M.S. Bhatti, Laminar convective heat transfer in ducts, in: S. Kakac,R.K. Shah, W. Aung (Eds.), *Handbook of Single – Phase Convective Heat Transfer*, Wiley, New York, (1987) .

**NUMENCLATURE**

$\bar{q}$	Heat flux W/m <sup>2</sup>	Pa
$\Delta p$	Pressure drop	
F	Friction factor	
DW	Distilled Water	
EG	Ethylene Glycol	
$k_n$	Thermal conductivity of Nano fluid	W/m <sup>2</sup> .k
$\Phi$	Nano particle volume fraction	
$\tau$	Shear stress	Pa
Ra	Rayleigh number	
$\gamma$	Shear rate	s <sup>-1</sup>

**Creek letters**

$\mu_n$	Dynamic viscosity Nano fluid	N.s/m <sup>2</sup>
$\rho_n$	Density of Nano fluid	kg/m <sup>3</sup>

**Subscripts**

n	Nanofluid
b	Base fluid